V-BLAST: An Architecture for Realizing Very High Data Rates Over the Rich-Scattering Wireless Channel

P. W. Wolniansky, G. J. Foschini, G. D. Golden, R. A. Valenzuela
Bell Laboratories, Lucent Technologies, Crawford Hill Laboratory
791 Holmdel-Keyport Rd., Holmdel, NJ 07733

ABSTRACT

Recent information theory research has shown that the rich-scattering wireless channel is capable of enormous theoretical capacities if the multipath is properly exploited. In this paper, we describe a wireless communication architecture known as vertical BLAST (Bell Laboratories Layered Space-Time) or V-BLAST, which has been implemented in realtime in the laboratory. Using our laboratory prototype, we have demonstrated spectral efficiencies of 20 - 40 bps/Hz in an indoor propagation environment at realistic SNRs and error rates. To the best of our knowledge, wireless spectral efficiencies of this magnitude are unprecedented, and are furthermore unattainable using traditional techniques.

1. INTRODUCTION

In the past few years, theoretical investigations have revealed that the multipath wireless channel is capable of enormous capacities, provided that the multipath scattering is sufficiently rich and is properly exploited through the use of an appropriate processing architecture [1-4]. The diagonally-layered space-time architecture proposed by Foschini [1], now known as diagonal BLAST (Bell Laboratories Layered Space-Time) or D-BLAST, is one such approach. D-BLAST utilizes multi-element antenna arrays at both transmitter and receiver and an elegant diagonally-layered coding structure in which code blocks are dispersed across diagonals in space-time. In an independent Rayleigh scattering environment, this processing structure leads to theoretical rates which grow linearly with the number of antennas (assuming equal numbers of transmit and receive antennas) with these rates approaching 90% of Shannon capacity.

However, the diagonal approach suffers from certain implementation complexities which make it inappropriate for initial implementation. In this paper, we describe a simplified version of BLAST known as vertical BLAST or V-BLAST, which has been implemented in realtime in the laboratory. Using our laboratory prototype, we have demonstrated spectral efficiencies of 20 - 40 bps/Hz at average SNRs ranging from 24 to 34 dB. Although these results were obtained in a relatively benign indoor environment, we believe that spectral efficiencies of this magnitude are unprecedented, regardless of propagation environment or SNR, and are simply unattainable using traditional techniques.

2. SYSTEM OVERVIEW

A high-level block diagram of a BLAST system is shown in Fig. 1. A single data stream is demultiplexed into M substreams, and each substream is then encoded into symbols and fed to its respective transmitter. (The encoding process is discussed in more detail below.) Transmitters $1 - M$ operate co-channel at symbol rate $1/T$ symbols/sec, with synchronized symbol timing. Each transmitter is itself an ordinary QAM transmitter. The collection of transmitters comprises, in effect, a vector-valued transmitter, where components of each transmitted M-vector are symbols drawn from a QAM constellation. We assume that the same constellation is used for each substream, and that transmissions are organized into bursts of L symbols. The power launched by each transmitter is proportional to $1/M$ so that the total radiated power is constant and independent of M.

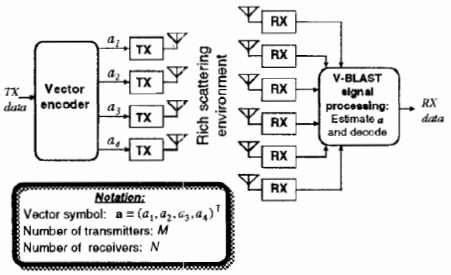

Figure 1: V-BLAST high level system diagram

The essential difference between D-BLAST and V-BLAST lies in the vector encoding process. In D-BLAST, redundancy between the substreams is introduced through the use of specialized inter-substream block coding. The D-BLAST code blocks are organized along diagonals in space-time. It is this coding that leads to D-BLAST's higher spectral efficiencies for a given number of transmitters and receivers. In V-BLAST, however, the vector encoding process is simply a demultiplex operation followed by independent bit-to-symbol mapping of each substream. No inter-substream coding, or coding of any kind, is required, though conventional coding of the individual substreams may certainly be applied. For the remainder of this paper, we will assume for

0-7803-4900-8/98/$10.00 © 1998 IEEE

simplicity that the substreams comprise uncoded, independent data symbols.

Receivers $1 - N$ are, individually, conventional QAM receivers. These receivers also operate co-channel, each receiving the signals radiated from all M transmit antennas. For simplicity in the sequel, flat fading is assumed, and the matrix channel transfer function is $\mathbf{H}^{N\times M}$, where h_{ij} is the (complex) transfer function from transmitter j to receiver i, and $M \leq N$. We take the quasi-stationary viewpoint that the channel time variation is negligible over the L symbol periods comprising a burst, and that the channel is estimated accurately, e.g. by use of a training sequence embedded in each burst; thus, for brevity in the remainder of the paper, we will not make the distinction between $\mathbf{H}$ and its estimate.

Although V-BLAST, as shown above, is essentially a single-user system which uses multiple transmitters, one can naturally ask in what ways the BLAST approach differs from simply using traditional multiple access techniques in a single-user fashion, i.e. by driving all the transmitters from a single user's data which has been split into substreams. Some of these differences are worth pointing out: First, unlike code-division or other spread-spectrum multiple access techniques, the total channel bandwidth utilized in a BLAST system is only a small fraction in excess of the symbol rate, i.e. similar to the excess bandwidth required by a conventional QAM system. Second, unlike FDMA, each transmitted signal occupies the entire system bandwidth. Finally, unlike TDMA, the entire system bandwidth is used simultaneously by all of the transmitters all of the time.

Taken together, these differences together are precisely what give BLAST the potential to realize higher spectral efficiencies than the multiple-access techniques. In fact, an essential feature of BLAST is that no explicit orthogonalization of the transmitted signals is imposed by the transmit structure at all. Instead, the propagation environment itself, which is assumed to exhibit significant multipath, is exploited to achieve the signal decorrelation necessary to separate the co-channel signals. V-BLAST utilizes a combination of old and new detection techniques to separate the signals in an efficient manner, permitting operation at significant fractions of the Shannon capacity and achieving large spectral efficiencies in the process.

3. V-BLAST DETECTION

In what follows, we take a discrete-time baseband view of the detection process for a single transmitted vector symbol, assuming symbol-synchronous receiver sampling and ideal timing. Letting $\mathbf{a} = (a_1, a_2, \cdots, a_M)^{\mathsf{T}}$ denote the vector of transmit symbols, then the corresponding received N-vector is

$$\mathbf{r}_1 = \mathbf{H}\mathbf{a} + \mathbf{v} \tag{1}$$

where $\mathbf{v}$ is a noise vector with components drawn from IID wide-sense stationary processes with variance σ^2.

One way to perform detection for this system is by using conventional adaptive antenna array (AAA) techniques, i.e. linear combinatorial nulling [6]: Conceptually, each substream in turn is considered to be the desired signal, and the remainder are considered as "interferers". Nulling is performed by linearly weighting the received signals so as to satisfy some performance-related criterion, such as minimum mean-squared error (MMSE) or zero-forcing (ZF).

For example, zero-forcing nulling can be performed by choosing weight vectors $\mathbf{w}_i$, $i = 1, 2, \cdots, M$, such that

$$\mathbf{w}_i^{\mathsf{T}}(\mathbf{H})_j = \delta_{ij} \tag{2}$$

where $(\mathbf{H})_j$ is the j-th column of $\mathbf{H}$, and δ is the Kronecker delta. Thus, the decision statistic for the i–th substream is $y_i = \mathbf{w}_i^{\mathsf{T}}\mathbf{r}_1$.

This linear nulling approach is viable, but superior performance is obtained if nonlinear techniques are used. One particularly attractive nonlinear alternative is to exploit the timing synchronism inherent in the system model (the assumption of co-located transmitters makes this completely reasonable) and use *symbol cancellation* as well as linear nulling to perform detection. Using symbol cancellation, interference from already-detected components of $\mathbf{a}$ is subtracted out from the received signal vector, resulting in a modified received vector in which, effectively, fewer interferers are present. This is somewhat analogous to decision feedback equalization.

When symbol cancellation is used, the order in which the components of $\mathbf{a}$ are detected becomes important to the overall performance of the system. Later, we will show how to determine a particular ordering which is optimal in a certain sense; for now, we first discuss the general detection procedure with respect to an arbitrary ordering.

Let the ordered set

$$S \equiv \{k_1, k_2, \cdots, k_M\} \tag{3}$$

be a permutation of the integers $1, 2, \cdots, M$ specifying the order in which components of the transmitted symbol vector $\mathbf{a}$ are extracted. The detection process proceeds generally as follows:

Step 1: Using nulling vector $\mathbf{w}_{k_1}$, form decision statistic y_{k_1}:

$$y_{k_1} = \mathbf{w}_{k_1}^{\mathsf{T}}\mathbf{r}_1 \tag{4}$$

Step 2: Slice y_{k_1} to obtain $\hat{a}_{k_1}$:

$$\hat{a}_{k_1} = Q(y_{k_1}) \tag{5}$$

where $Q(\cdot)$ denotes the quantization (slicing) operation appropriate to the constellation in use.

Step 3: Assuming that $\hat{a}_{k_1} = a_{k_1}$, cancel a_{k_1} from the received vector $\mathbf{r}_1$, resulting in modified received vector $\mathbf{r}_2$:

$$\mathbf{r}_2 = \mathbf{r}_1 - \hat{a}_{k_1}(\mathbf{H})_{k_1} \tag{6}$$

where $(\mathbf{H})_{k_1}$ denotes the k_1-th column of $\mathbf{H}$. Steps 1 - 3 are then performed for components $k_2, \cdots, k_M$ by operating in turn on the progression of modified received vectors $\mathbf{r}_2, \mathbf{r}_3, \cdots, \mathbf{r}_M$.

The specifics of the detection process depend on the criterion chosen to compute the nulling vectors $\mathbf{w}_{k_i}$, the most common of these being MMSE or ZF. The detection process is described here with respect to the ZF criterion since it is somewhat simpler to state. The k_i-th ZF-nulling vector is defined as the unique minimum norm vector satisfying

$$\mathbf{w}_{k_i}^{\mathrm{T}}(\mathbf{H})_{k_j} = \begin{cases} 0 & j \geq i \\ 1 & j = i \end{cases} . \tag{7}$$

Thus, $\mathbf{w}_{k_i}$ is orthogonal to the subspace spanned by the contributions to $\mathbf{r}_i$ due to those symbols not yet estimated and cancelled. It is not difficult to show that the unique vector satisfying (7) is just the k_i-th row of $\mathbf{H}_{k_{i-1}}^{+}$ where the notation $\mathbf{H}_{\bar{k}_i}$ denotes the matrix obtained by zeroing columns $k_1, k_2, \cdots, k_i$ of $\mathbf{H}$ and $^{+}$ denotes the Moore-Penrose pseudoinverse [5].

The post-detection SNR for the k_i-th detected component of $\mathbf{a}$ is easily obtained by substituting (1) and (7) into (4), and taking expected values, i.e.

$$\rho_{k_i} = \frac{<|a_{k_i}|^2>}{\sigma^2 \|\mathbf{w}_{k_i}\|^2} \tag{8}$$

where the expectation in the numerator is taken over the constellation set.

3.1 OPTIMAL DETECTION ORDERING

As mentioned earlier, when symbol cancellation is used, the system performance is affected by the order in which the components of $\mathbf{a}$ are detected, whereas it does not matter when pure nulling is used. In order to appreciate this, first consider why it is that nulling with cancellation performs better than pure nulling, regardless of ordering.

When nulling alone is used, each nulling vector is required, according to (2), to be orthogonal to $M - 1$ rows of $\mathbf{H}$. However, when symbol cancellation is employed in addition to nulling, $\mathbf{w}_{k_i}$ is required to be orthogonal only to the $M - i$ undetected components as per (7). A simple consequence of the Cauchy-Schwartz inequality is that the more rows of $\mathbf{H}$ that a particular $\mathbf{w}_{k_i}$ is constrained to be orthogonal to, the larger its norm, and thus, according to (8), the smaller its post-detection SNR. When using cancellation then, the ρ_{k_i} are lower bounded (with equality only for ρ_{k_1}) by their corresponding nulling-only ρ_{k_i}.

The importance of ordering is simply that it permits, during the detection of the i-th component, a choice as to *which* subset of $M - i$ rows that $\mathbf{w}_{k_i}$ should be constrained by; different choices lead to different ρ_{k_i}. For example, in an $M = 3$ system, detecting component 1 first (in the presence of 2 and 3) will, in general, result in a different ρ_1 than if component 2 was detected first (in the presence of 1 and 3). With pure nulling, each component is always detected in the presence of all the others, so ordering does not matter.

Now recall that all components of $\mathbf{a}$ are assumed to utilize the same constellation. Under this assumption, the component with the smallest ρ_{k_i} will dominate the error performance of the system. Thus, an obvious figure of merit for this system - though not the only one possible - is the maximization of the worst, i.e. the minimum, of the ρ_{k_i} over all possible detection orderings. A surprising result - and one which we believe has not been previously appreciated - is that simply choosing the best ρ_{k_i} *at each stage in the detection process* leads to the globally optimum ordering, S_{opt}, in this maximin sense. The proof is given in the appendix.

We remark that this optimality result may have wider applicability to multi-user cancellation-based detection as well. Although the "best first" cancellation approach is widely known within the multi-user community [7-8], essentially being the defacto approach, we are not aware of any previous proof of its optimality in the sense given here.

The full ZF V-BLAST detection algorithm can now be described compactly as a recursive procedure, including determination of the optimal ordering, as follows:

initialization:

$$i \leftarrow 1 \tag{9a}$$
$$\mathbf{G}_1 = \mathbf{H}^{+} \tag{9b}$$
$$k_1 = \underset{j}{\operatorname{argmin}} \|(\mathbf{G}_1)_j\|^2 \tag{9c}$$

recursion:

$$\mathbf{w}_{k_i} = (\mathbf{G}_i)_{k_i} \tag{9d}$$
$$y_{k_i} = \mathbf{w}_{k_i}^{\mathrm{T}} \mathbf{r}_i \tag{9e}$$
$$\hat{a}_{k_i} = Q(y_{k_i}) \tag{9f}$$
$$\mathbf{r}_{i+1} = \mathbf{r}_i - \hat{a}_{k_i}(\mathbf{H})_{k_i} \tag{9g}$$
$$\mathbf{G}_{i+1} = \mathbf{H}_{\bar{k}_i}^{+} \tag{9h}$$
$$k_{i+1} = \underset{j \notin \{k_1 \cdots k_i\}}{\operatorname{argmin}} \|(\mathbf{G}_{i+1})_j\|^2 \tag{9i}$$
$$i \leftarrow i + 1 \tag{9j}$$

where $(\mathbf{G}_i)_j$ is the j-th row of $\mathbf{G}_i$. Thus, (9c,i) determine the elements of S_{opt}, the optimal ordering; (9d-f) compute respectively the ZF-nulling vector, the decision statistic, and the estimated component of **a**; (9g) performs cancellation of the detected component from the received vector, and (9h) computes the new pseudoinverse for the next iteration. Note that this new pseudoinverse is based on a "deflated" version of **H**, in which columns $k_1, k_2, \cdots, k_i$ have been zeroed. This is because these columns correspond to components of **a** which have already been estimated and cancelled, and thus the system becomes equivalent to a "deflated" version of Fig. 1 in which transmitters $k_1, k_2, \cdots, k_i$ have been removed, or equivalently, a system in which $a_{k_1} = \cdots = a_{k_i} = 0$.

4. LABORATORY RESULTS

A laboratory prototype of a V-BLAST system has been constructed for the purpose of demonstrating the feasibility of the BLAST approach. The prototype operates at a carrier frequency of 1.9 GHz, and a symbol rate of 24.3 ksymbols/sec, in a bandwidth of 30 kHz. The receiver processing is similar to that shown in (9).

The system was operated and characterized in the actual laboratory/office environment, not a test range, with transmitter and receiver separations up to about 12 meters. This environment is relatively benign in that the delay spread is negligible, the fading rates are low, and there is significant near-field scattering from nearby equipment and office furniture. Nevertheless, it is a representative indoor lab/office situation, and no attempt was made to "tune" the system to the environment, or to modify the environment in any way.

The antenna arrays consisted of λ/2 wire dipoles mounted in various arrangements. For the results shown below, the receive dipoles were mounted on the surface of a metallic hemisphere approximately 20 cm in diameter, and the transmit dipoles were mounted on a flat metal sheet, in a roughly rectangular array with about λ/2 inter-element spacing. In general, the system performance was found to be nearly independent of small details of the array geometry.

Fig. 2 shows results obtained with the prototype system, using $M = 8$ transmitters and $N = 12$ receivers. In this experiment, the transmit and receive arrays were each placed at a single representative position within the environment, and the performance characterized. The horizontal axis is spatially averaged received SNR, i.e., $\frac{1}{N}\sum_{i=1}^{N} SNR_i$, where SNR_i is the the ratio of received signal power (from all M transmitters) to noise power at the i-th receiver. The vertical axis is the block error rate, where a "block" is defined as a single transmission burst. In this case, the burst length L is 100 symbol durations, 20 of which are used for training. In this experiment, each of the eight substreams utilized uncoded 16-QAM, i.e. 4 bits/symbol/transmitter, so that the payload block size is 8×4×80 = 2560 bits. The raw spectral efficiency of this configuration is thus

$$E_s = \frac{(8\text{xmtrs})\times(4\text{b/sym/xmtr})\times(24.3\text{ksym/s})}{30\text{kHz}} = 25.9 \text{ bps/Hz}$$

and the payload efficiency is 80% of the above, or 20.7 bps/Hz, corresponding to a payload data rate of 621 kbps in 30 kHz bandwidth.

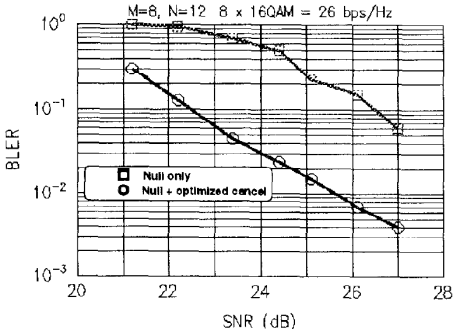

Figure 2: Single-position performance

The upper curve in Fig. 2 shows performance obtained when conventional nulling is used. The lower curve shows performance using nulling and optimally-ordered cancellation. The average difference is about 4 dB, which corresponds to a raw spectral efficiency differential (for this configuration) of around 10 bps/Hz.

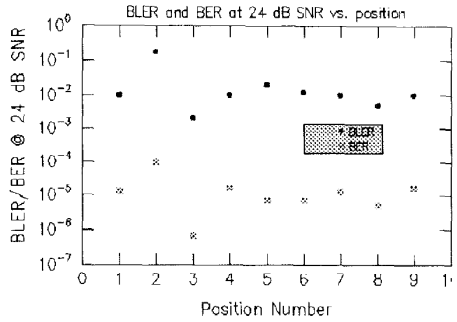

Figure 3: Multiple-position performance

Figure 3 shows performance results obtained using the same BLAST system configuration ($M = 8$, $N = 12$, 16-QAM) when the receive array was left fixed and the transmit array was located at different positions throughout the environment. In each case,

the transmit power was adjusted so that the average received SNR was 24±0.5 dB. Nulling with optimized cancellation was used.

It can be seen that operation at this spectral efficiency is reasonably robust with respect to antenna position. In all positions, the system had at least 2 orders of magnitude margin relative to 10^{-2} BER. For a completely uncoded system, these are entirely reasonable error rates, and application of ordinary error correcting codes would significantly reduce this. At 34 dB SNR, spectral efficiencies as high as 40 bps/Hz have been demonstrated at similar error rates, though with less robust performance.

We believe these spectral efficiencies to be unprecedented for the wireless channel. It is worthwhile to point out that spectral efficiencies of these magnitudes are essentially impossible to obtain using traditional approaches in which a single transmitter is used, simply because the required constellation loadings would be immense. For example, to obtain the equivalent of the 32 bits per vector symbol in the experiments above, but using a single transmitter, would require a constellation with 2^{32} or more than a billion (10^9) points, which seems well outside of the realm of practicality, regardless of SNR.

SUMMARY AND CONCLUSIONS

We have described V-BLAST, a wireless architecture capable of realizing extraordinary spectral efficiencies over the rich-scattering wireless channel. The general BLAST approach and the V-BLAST detection scheme were motivated and described in detail, and an interesting new optimality result regarding cancellation-based detection (which may have wider applicability to multi-user detection as well) was reported. Early results with our V-BLAST realtime laboratory prototype have proven the feasibility of the concept, and we have demonstrated spectral efficiencies of 20 - 40 bps/Hz under real-world indoor conditions, exceeding any results that we are aware of using traditional modulation techniques. Although these results were obtained in a relatively benign environment, we are nevertheless strongly encouraged, and believe that the BLAST approach may eventually lead to significantly improved spectral efficiencies in wireless systems.

APPENDIX: PROOF OF THE OPTIMALITY OF ORDERING IMPOSED BY EQ. (9)

Definitions and notation:

For a given detection ordering $\mathcal{S} \equiv \{S_1, S_2, \cdots, S_M\}$ define the *constraint set* of S_i to be the set $\{S_{i+1}, S_{i+2}, \cdots, S_M\}$, or the null set if $i = M$. The constraint set is just those components of $\mathbf{a}$ which have not yet been detected and cancelled.

Let $\mathcal{S}$ be a detection ordering. Then define ρ_{S_i} to be the post-detection SNR at the i-th stage of the detection process when using this ordering, i.e. ρ_{S_i} is the post-detection SNR when detecting a_{S_i} according to (9e).

Let $\mathcal{L} \equiv \{L_1, L_2, \cdots, L_M\}$ be the locally-optimum ordering obtained using (9).

The following trivial lemmas are used in what follows and are stated here without proof:

Lemma 1: Let $\mathcal{A}$ and $\mathcal{B}$ be two distinct orderings. If $A_k = B_k$, and the constraint sets of A_k and B_k consist of identical elements (regardless of their order), then $\rho_{A_k} = \rho_{B_k}$.

Lemma 2: Let $\mathcal{A}$ and $\mathcal{B}$ be two distinct orderings. If $A_k = B_k$, and the constraint set of A_k is a subset of the constraint set of B_k, then $\rho_{A_k} \geq \rho_{B_k}$.

Proof:

Let $\mathcal{Q} \equiv \{Q_1, Q_2, \cdots, Q_M\}$ be an arbitrary ordering distinct from $\mathcal{L}$. Let d be the index of the first (leftmost) element for which $\mathcal{L}$ and $\mathcal{Q}$ differ. Let r be the index for which $Q_r = L_d$. (Note that $r > d$, since $\mathcal{L}$ and $\mathcal{Q}$ have common elements up to index $d-1$.) By Lemma 1,

$$\rho_{L_i} = \rho_{Q_i} \qquad 1 \leq i \leq d-1 . \quad \text{(A.1)}$$

Now define $\mathcal{Q}'$ to be a perturbation of $\mathcal{Q}$ obtained by moving Q_r from index r to index d, and "squeezing" the rest of $\mathcal{Q}$ so that the elements of $\mathcal{Q}'$ are

$$\mathcal{Q}' = \{Q_1, Q_2, \cdots, Q_{d-1}, Q_r, Q_d, \ldots, Q_M\}$$

where it is understood that the sequence above Q_d is actually "missing" the repositioned Q_r element. Note that $\mathcal{Q}'$ matches $\mathcal{L}$ in the first d positions, whereas $\mathcal{Q}$ matches $\mathcal{L}$ only in the first $d-1$ positions.

Now consider the post-detection SNRs that would result from using $\mathcal{Q}'$ instead of $\mathcal{Q}$:

By Lemma 1, $\rho_{Q_1} = \rho_{Q'_1}$, $\rho_{Q_2} = \rho_{Q'_2}, \cdots, \rho_{Q_{d-1}} = \rho_{Q'_{d-1}}$, since these elements have the same constraint sets.

By either Lemma 1 or Lemma 2, $\rho_{Q_{d+1}} \leq \rho_{Q'_{d+1}}$, $\rho_{Q_{d+2}} \leq \rho_{Q'_{d+2}}, \cdots, \rho_{Q_M} \leq \rho_{Q'_M}$, since these elements either have the same constraint sets, or the constraint set of the $\mathcal{Q}'$ elements are subsets of the constraint sets of the corresponding $\mathcal{Q}$ elements.

Finally, $\rho_{Q_d} \leq \rho_{Q'_d}$, since $\rho_{Q'_d} = \rho_{L_d}$ and ρ_{L_d} is, by virtue of the local maximization procedure (9), at least as large as any other choice in that position. Thus,

$$\min_i \rho_{Q_i} \leq \min_i \rho_{Q'_i} \quad \text{(A.2)}$$

An obvious inductive argument allows that by successive similar perturbations, $\mathcal{Q}$ can be transformed

DOCKET ALARM

Explore Litigation Insights

Docket Alarm provides insights to develop a more informed litigation strategy and the peace of mind of knowing you're on top of things.

Real-Time Litigation Alerts

Keep your litigation team up-to-date with **real-time alerts** and advanced team management tools built for the enterprise, all while greatly reducing PACER spend.

Our comprehensive service means we can handle Federal, State, and Administrative courts across the country.

Advanced Docket Research

With over 230 million records, Docket Alarm's cloud-native docket research platform finds what other services can't. Coverage includes Federal, State, plus PTAB, TTAB, ITC and NLRB decisions, all in one place.

Identify arguments that have been successful in the past with full text, pinpoint searching. Link to case law cited within any court document via Fastcase.

Analytics At Your Fingertips

Learn what happened the last time a particular judge, opposing counsel or company faced cases similar to yours.

Advanced out-of-the-box PTAB and TTAB analytics are always at your fingertips.

API

Docket Alarm offers a powerful API (application programming interface) to developers that want to integrate case filings into their apps.

LAW FIRMS
Build custom dashboards for your attorneys and clients with live data direct from the court.

Automate many repetitive legal tasks like conflict checks, document management, and marketing.

FINANCIAL INSTITUTIONS
Litigation and bankruptcy checks for companies and debtors.

E-DISCOVERY AND LEGAL VENDORS
Sync your system to PACER to automate legal marketing.